Appl. Phys. B 74, 705–709 (2002)
DOI: 10.1007/s003400200841

Applied Physics B
Lasers and Optics

N.N. DADOENKOVA✉
T. ANDERSEN
W. HÜBNER

Nonlinear surface magneto-optics of ferromagnetic Ni/Cu(001) from first principles

Max-Planck-Institut für Mikrostrukturphysik, Weinberg 2, 06120 Halle (Saale), Germany

Received: 16 October 2001/Revised version: 8 March 2002
Published online: 29 May 2002 • © Springer-Verlag 2002

ABSTRACT We present first-principles calculations of the nonlinear optical (NLO) response of a Ni/Cu(001) bilayer. The calculations are based on the full potential linearized augmented plane wave (FLAPW) method with the additional implementation of spin–orbit coupling (SOC). On the basis of this set of eigenstates the magneto-optical transition-matrix elements are evaluated. Using the surface-sheet model the optical reflection properties are determined for the cases of the magnetization vector perpendicular to the surface (polar magneto-optical configuration (MOC)) and for the in-plane magnetization (longitudinal MOC). The nonlinear optical susceptibility tensor elements $\chi_{ijk}^{(2)}$ for different magnetization directions as well as the spectral dependence of $\chi_{ijk}^{(2)}$, the resulting intensities, and Kerr angles are presented for the Ni/Cu(001) bilayer. The results show that the magnetic tensor elements of the $\chi_{ijk}^{(2)}$ tensor are smaller than the nonmagnetic ones by only one order of magnitude, confirming the important role of magnetic properties in the NLO response.

PACS 78.20.Ls; 73.20.At;78.66.Bz

1 Introduction

Nonlinear magneto-optical techniques are powerful tools for the spectroscopic investigation of thin-film systems and represent an intensely developing branch of modern optics [1]. It is well known that the electric-dipole contribution is forbidden in the bulk of centrosymmetric materials. Due to the inversion-symmetry breaking at the interfaces and surfaces, the second-order magneto-optical response demonstrates surface and interface sensitivity. Recently, considerable attention has been paid to the investigation of nonlinear magneto-optical effects for various magnetic materials, especially thin magnetic films and multilayered structures [2–10]. Moreover, the nonlinear magneto-optical Kerr effect (NOLIMOKE) combines surface and interface sensitivity with large magneto-optical effects, which usually are about one to two orders of magnitude larger than their linear analogues [1, 2], and for some geometries can achieve an enhancement by almost three orders of magnitude (e.g. the nonlinear Kerr rotation of Fe (2 nm)/Cr (3 nm) multilayers [3]). In addition the theoretical predictions of the nonlinear Kerr effect at the surfaces [11, 12] were confirmed experimentally in numerous works for surfaces, as well for multilayer interfaces [8–10]. This fact makes magnetically induced second-harmonic generation (MSHG) a very attractive method for the probing of surface and interface magnetism of ultrathin magnetic films, multilayers, and superlattices [7–10, 13–17], especially where the linear Kerr rotation is vanishingly small. In the last few years NOLIMOKE earned recognition as a technique of high efficiency in magnetic imaging for the visualization of magnetic domains and domain walls [1, 7, 14, 18, 19]. MSHG allows to obtain unique information about the domain structure in antiferromagnetic materials as well [1].

The electronic theory of the nonlinear magneto-optical response and NOLIMOKE was proposed [12] and developed for transition metals such as Fe and Ni [20–23]. The linear and nonlinear magneto-optical Kerr effects result from the combined action of spin–orbit coupling (SOC) and the exchange interaction. At first, the SOC was treated perturbatively [22], but later it was included from first principles for the calculation of nonlinear optical susceptibility tensor elements of free-standing fcc Fe monolayers [5, 6].

In this article, we present calculations of the NLO response and Kerr rotation for the fcc Ni/Cu(001) bilayer, including spin-polarization, SOC, and dipole transition-matrix elements calculated from first principles. Both the longitudinal and polar magneto-optical configurations (MOCs) are considered since, experimentally, the easy axis of one Fe monolayer on Cu(001) is perpendicular to the film plane, while it lies in-plane for one monolayer of Ni on Cu(001) [24, 25]. Here, besides the in-plane magnetized Ni/Cu(001) system, we present calculations for the out-of-plane magnetized Ni/Cu(001) bilayer in order to compare with the Fe/Cu(001) results previously obtained in the same nonlinear MOC [the ground state of Fe/Cu(001)].

2 Theory

First, we consider an fcc Ni/Cu(001) bilayer which is located in the $\boldsymbol{xy}$ plane with the $\boldsymbol{z}$ axis perpendicular to the surface. The $\boldsymbol{x}$ and $\boldsymbol{y}$ axes coincide with the crystallographical directions [100] and [010], respectively.

✉ E-mail: ndadoenk@mpi-halle.de; danata@kinetic.ac.donetsk.ua

The calculation of the screened nonlinear magneto-optical response, characterized by the nonlinear optical susceptibility tensor $\chi^{(2)}_{ijk}(2\boldsymbol{q}, 2\omega)$, is based on the formula derived in [12]:

$$\begin{aligned}\chi^{(2)}_{ijk}(2\boldsymbol{q}, 2\omega) = e^3 \sum_{\boldsymbol{k},l,l',l''} \Bigg\{ &\langle \boldsymbol{k}+2\boldsymbol{q}, l''|\boldsymbol{r}_i|\boldsymbol{k}, l\rangle\langle \boldsymbol{k}, l|\boldsymbol{r}_j|\boldsymbol{k}+\boldsymbol{q}, l'\rangle \\ &\times \frac{\langle \boldsymbol{k}+\boldsymbol{q}, l'|\boldsymbol{r}_k|\boldsymbol{k}+2\boldsymbol{q}, l''\rangle}{E_{\boldsymbol{k}+2\boldsymbol{q},l''} - E_{\boldsymbol{k},l} - 2\hbar\omega + 2\mathrm{i}\hbar\alpha} \\ &\times \left(\frac{f(E_{\boldsymbol{k}+2\boldsymbol{q},l''}) - f(E_{\boldsymbol{k}+\boldsymbol{q},l'})}{E_{\boldsymbol{k}+2\boldsymbol{q},l''} - E_{\boldsymbol{k}+\boldsymbol{q},l'} - \hbar\omega + \mathrm{i}\hbar\alpha} \right. \\ &\left. - \frac{f(E_{\boldsymbol{k}+\boldsymbol{q},l'}) - f(E_{\boldsymbol{k},l})}{E_{\boldsymbol{k}+\boldsymbol{q},l'} - E_{\boldsymbol{k},l} - \hbar\omega + \mathrm{i}\hbar\alpha} \right) \Bigg\} \\ &\times \Bigg[1 + 4\pi e^2 \sum_{ab} m_a m_b \\ &\times \sum_{\boldsymbol{k},l,l''} \langle \boldsymbol{k}, l\,|\boldsymbol{r}_a|\,\boldsymbol{k}+2\boldsymbol{q}, l''\rangle\langle \boldsymbol{k}+2\boldsymbol{q}, l''\,|\boldsymbol{r}_b|\,\boldsymbol{k}, l\rangle \\ &\times \frac{f(E_{\boldsymbol{k}+2\boldsymbol{q},l''}) - f(E_{\boldsymbol{k},l})}{E_{\boldsymbol{k}+2\boldsymbol{q},l''} - E_{\boldsymbol{k}l} - 2\hbar\omega + 2\mathrm{i}\hbar\alpha} \Bigg]^{-1} . \end{aligned} \quad (1)$$

Here, $\boldsymbol{q}$ and ω are the wave vector and the frequency of the incident light, the $E_{\boldsymbol{k},l}$ are the energy bands, corresponding to the quantum states $|\boldsymbol{k}, l\rangle$, α is a damping constant, $f(E_{\boldsymbol{k},l})$ is the Fermi distribution, and $m_{a,b}$ are the direction cosines between $\boldsymbol{q}$ and the coordinate axes a, b. The dipole-matrix elements in (1) employ the wave functions $|\boldsymbol{k}, l\rangle$, which are obtained by the full potential linearized augmented plane wave (FLAPW) method implemented in the package WIEN97 [26] on the basis of density-functional theory within the generalized gradient approximation (GGA). For the bilayer a supercell approach has been used because of the need for translational invariance in the z direction in WIEN97. SOC is included in the second variational treatment. For the construction of the supercell for the Ni/Cu(001) bilayer we use 10 Cu-lattice spacings in the z direction to provide electronic decoupling between neighboring films in the supercell.

The calculations of the second-harmonic electric field are based on the surface-sheet model [27]. The particular expression for the second-harmonic electric field is given in [4].

3 Discussion and results

We assume pseudomorphic film growth and use lattice constants for both systems equal to that of bulk Cu, which is 3.61 Å. For the calculation of the band structure $E_{\boldsymbol{k},l'}$ and wave functions $|\boldsymbol{k}, l\rangle$, the total energy was converged to better than 10^{-4} Ry. According to [4–6], SOC is treated inside the muffin-tin spheres only and we choose a muffin-tin radius of 1.21 Å both for the Ni and the Cu atoms.

For the polar MOC the tensor $\chi^{(2)}_{ijk}$ has the following form:

$$\chi^{(2)}_{ijk} = \left(\begin{array}{ccc|ccc} 0 & 0 & 0 & \chi^{(-)}_{xyz} & \chi^{(+)}_{xxz} & 0 \\ 0 & 0 & 0 & \chi^{(+)}_{xxz} & -\chi^{(-)}_{xyz} & 0 \\ \chi^{(+)}_{zxx} & \chi^{(+)}_{zxx} & \chi^{(+)}_{zzz} & 0 & 0 & 0 \end{array} \right), \quad (2)$$

with only four independent elements $\chi^{(+)}_{zxx}$, $\chi^{(+)}_{zzz}$, $\chi^{(+)}_{xxz}$, and $\chi^{(-)}_{xyz}$. For the magnetization vector along the $\boldsymbol{z}$ axis the directions $\boldsymbol{x}$ and $\boldsymbol{y}$ are equivalent, and the components $\chi^{(+)}_{zxx}$ and $\chi^{(+)}_{zyy}$ coincide. Here, superscripts $(-)$ and $(+)$ denote components that are odd and even under magnetization reversal. The $(+)$ components contain both crystallographic and magnetically induced parts while the $(-)$ components are exclusively of magnetic origin [18].

For the longitudinal MOC, $\chi^{(2)}_{ijk}$ reads:

$$\chi^{(2)}_{ijk} = \left(\begin{array}{ccc|ccc} 0 & 0 & 0 & 0 & \chi^{(+)}_{xxz} & \chi^{(-)}_{xxy} \\ \chi^{(-)}_{yxx} & \chi^{(-)}_{yyy} & \chi^{(-)}_{yzz} & \chi^{(+)}_{yyz} & 0 & 0 \\ \chi^{(+)}_{zxx} & \chi^{(+)}_{zyy} & \chi^{(+)}_{zzz} & \chi^{(-)}_{zyz} & 0 & 0 \end{array} \right). \quad (3)$$

Figure 1 demonstrates the spectral behavior of the real and imaginary parts of the nonzero independent components of the $\chi^{(2)}_{ijk}$ tensor for the polar MOC ($\boldsymbol{M} \parallel \boldsymbol{z}$) for the Ni/Cu(001) and Fe/Cu(001) bilayers. The data for the Fe/Cu(001) bilayer are taken from [4]. As one can see from Fig. 1, the values of the real and imaginary parts for the corresponding components of the $\chi^{(2)}_{ijk}$ tensor are of the same order of magnitude for both systems. In general, the odd tensor element is smaller by one order of magnitude. For Ni/Cu(001) the spectral dependence of the nonvanishing components of the $\chi^{(2)}_{ijk}$ tensor for the longitudinal MOC ($\boldsymbol{M} \parallel \boldsymbol{x}$) is depicted in Fig. 2. Since the even tensor elements are of the same order of magnitude as in the polar MOC of Fig. 1, one can see that the odd components of the nonlinear susceptibility tensor are again only one order of magnitude smaller. For some energy regions their values are comparable, however. This fact confirms the importance of magnetic properties in the NLO response.

We show SHG intensities for the four basic geometries: p- or s-polarized input light giving a P- or S-polarized SHG signal. We calculate SHG intensities for the angle of incidence equal to $\pi/4$ and azimuth $\gamma = 0$ (see equation (3) for the electric field at the SHG frequency in [4]). The azimuth γ is the angle between the optical plane and the direction of the $\boldsymbol{x}$ axis. The input electric field E_0 is taken to be equal to 10^8 V/m. The refractive index for Cu is taken from [28].

The orientation of the magnetization vector also affects the intensity spectra. The peculiarities of the intensity spectra are presented in Fig. 3, where the solid lines correspond to $\boldsymbol{M} \parallel \boldsymbol{x}$ and the dashed ones to $\boldsymbol{M} \parallel \boldsymbol{z}$. The change of the magnetization from out-of-plane to in-plane yields new visible peaks in the energy region between 7 and 7.5 eV for s- and p-input to S-output geometries. Especially evident differences in the intensity spectra are observed for the p-input to S-output geometry. In general, S-output SHG intensities are much weaker than P-output. The s- to S configuration gives no SHG signal for the polar MOC, as expected. It is remarkable that, except for the s to S case, the low-energy edge of the signal is mostly given by the onset of the Cu d-electron absorption.

In Fig. 4 we show the azimuthal dependence of the second-harmonic intensities generated by the Ni/Cu(001) bilayer with in-plane magnetization at an incident photon energy of 1.5 eV. For a P-polarized SHG signal and both p- and s-polarized incident light we observe a visible change of the azimuthal behavior upon magnetization reversal. Dashed lines in Fig. 4a and b correspond to $\boldsymbol{M} \parallel -\boldsymbol{x}$. By contrast, for the p-polarized incident light and S-output, the azimuthal dependence changes insignificantly under magnetization reversal ($\sim 10^{-9}$), and for s- to S-geometry it does not undergo any

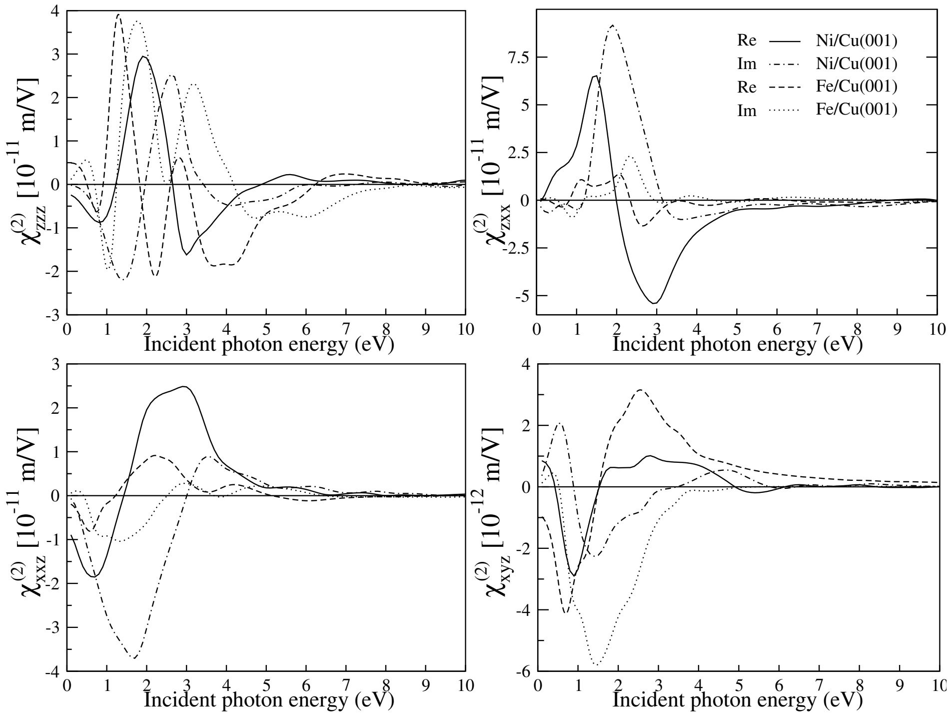

FIGURE 1 Spectral dependence of the nonlinear susceptibility tensor for the Ni/Cu(001) and Fe/Cu(001) bilayers with out-of-plane magnetization. The *solid* and *dash-dotted lines* correspond to the real and imaginary parts of the $\chi^{(2)}_{ijk}$ tensor for Ni/Cu(001); *dashed* and *dotted lines* depict real and imaginary parts of $\chi^{(2)}_{ijk}$ for the Fe/Cu(001) bilayer correspondingly

change at all (see Fig. 4c and d). This fact becomes clear if we examine which components of the $\chi^{(2)}_{ijk}$ tensor contribute to the corresponding polarization of the SHG field. For both p- and s-polarized input giving P-output, as well as for p-input to S-output, SHG involves results from linear combinations of both odd and even tensor elements, leading to an intensity change under magnetization reversal. In the case of incident s-polarized input and S-output light the situation is different. The S-polarized output SHG field results from the odd components $\chi^{(-)}_{yxx}$, $\chi^{(-)}_{yyy}$, and $\chi^{(-)}_{xxy}$ only, so the S-output intensity is the square of the odd components of the $\chi^{(2)}_{ijk}$ tensor alone, which does not change its value. For the case $\boldsymbol{M} \parallel \boldsymbol{z}$ the magnetization does not break the equivalence of the $\boldsymbol{x}$ and $\boldsymbol{y}$ directions at all and, as a result, the second-harmonic

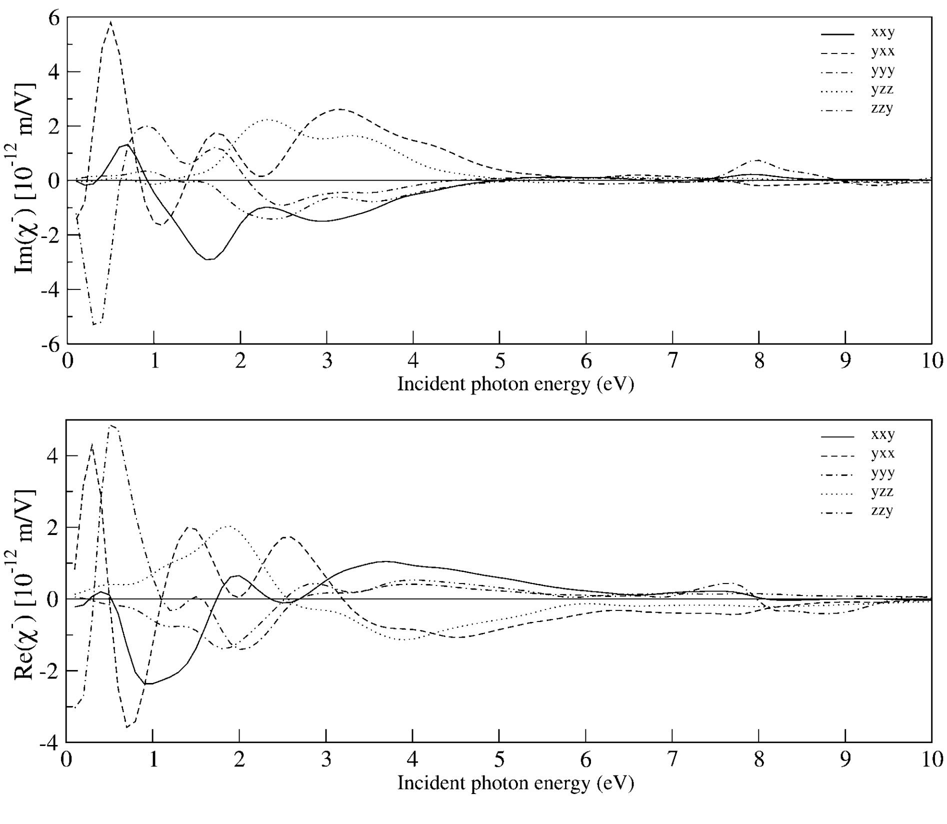

FIGURE 2 Spectral dependence of the odd (in magnetization) components of the χ_{ijk} tensor for the Ni/Cu(001) bilayer with the in-plane magnetization direction

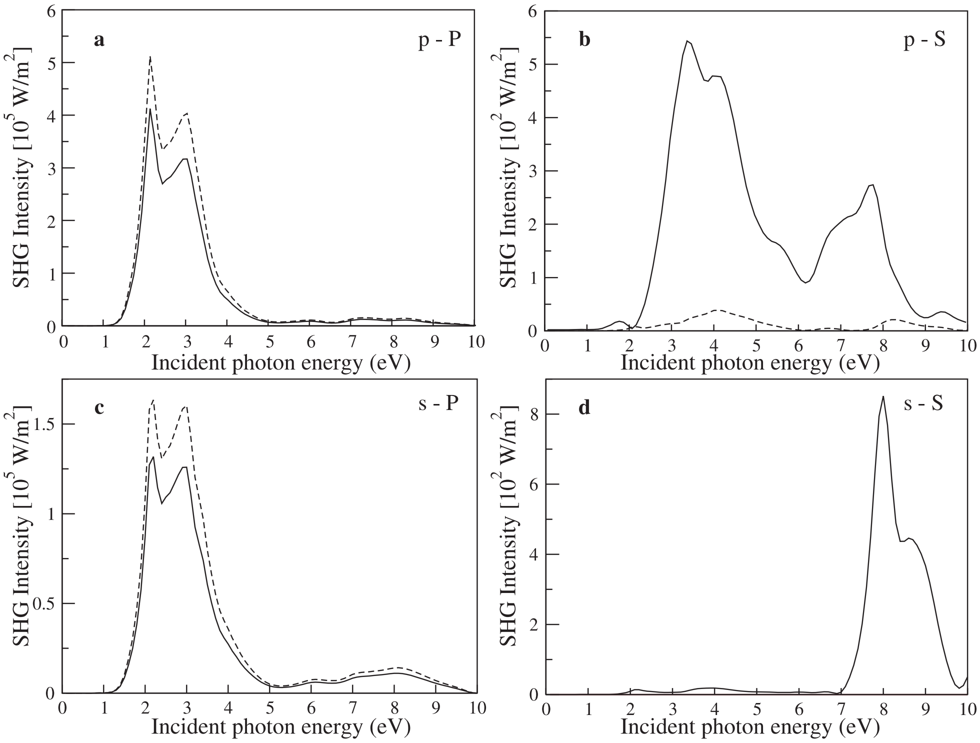

FIGURE 3 Intensities of SHG light generated by the Ni/Cu(001) bilayer with in-plane (*solid lines*) and out-of-plane (*dashed lines*) magnetization directions for: **a** *p*-polarized input light and *P*-polarized output, **b** *p*-polarized input light and *S*-polarized output, **c** *s*-polarized input light and *P*-polarized output, **d** *s*-polarized input light and *S*-polarized output

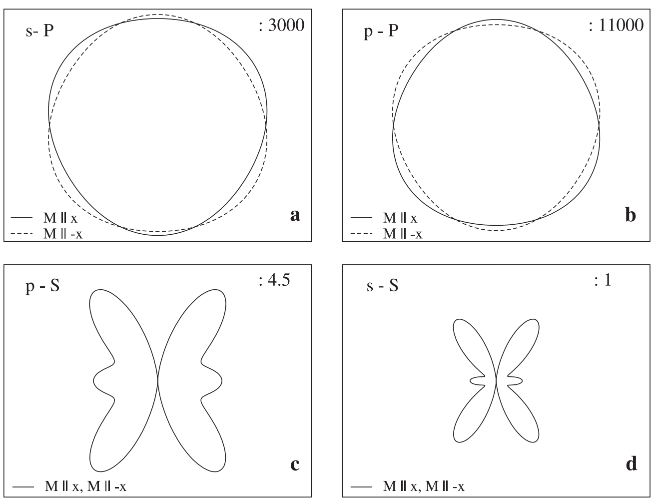

FIGURE 4 Azimuthal dependence of the nonlinear intensities for the Ni/Cu (001) bilayer with in-plane magnetization: **a** *p*-polarized input light and *P*-polarized output, **b** *p*-polarized input light and *S*-polarized output, **c** *s*-polarized input light and *P*-polarized output, **d** *s*-polarized input light and *S*-polarized output. *Solid lines* correspond to $\boldsymbol{M} \parallel \boldsymbol{x}$, *dashed lines* correspond to $\boldsymbol{M} \parallel -\boldsymbol{x}$

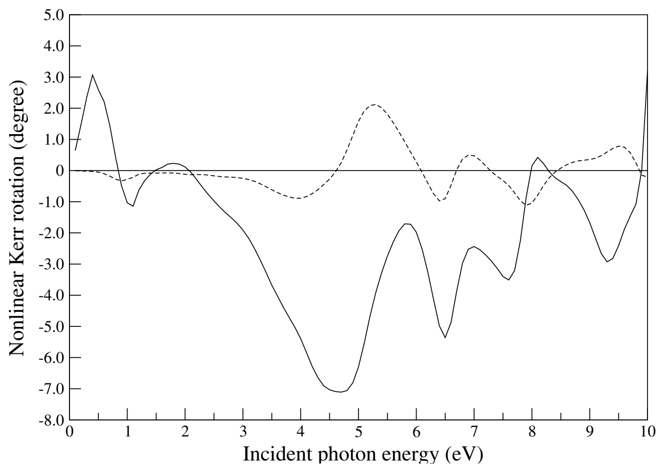

FIGURE 5 Dependence of the nonlinear Kerr rotation on the incident photon energy for the Ni/Cu(001) bilayer with in-plane (*solid line*) and out-of-plane (*dashed line*) magnetizations

intensities reveal no azimuthal dependence for all four geometries mentioned above. The analogous result was obtained in [5] for the freestanding Fe(001) monolayer with out-of-plane magnetization.

Figure 5 shows the dependence of the nonlinear Kerr rotation for the Ni/Cu(001) bilayer in the cases of polar and longitudinal MOCs with *p*-polarized incident light. The maximum nonlinear Kerr rotation for the out-of-plane magnetization is about 2°, at an incident photon energy of 5.2 eV. For the in-plane magnetization the maximum is shifted to 4.6 eV and reaches approximately −7.5°. These values of the Kerr rotations are obtained for an angle of incidence of $\pi/4$, and $\gamma = 0$. Thus, for the Ni/Cu(001) bilayer the NOLIMOKE rotation is two orders of magnitude larger than the linear magneto-optical Kerr effect.

4 Conclusions

We have presented first-principles calculations of nonlinear magneto-optical effects for the Ni/Cu(001) bilayer, using the FLAPW method with the additional implementation of the SOC. Our results confirm the enhanced sensitivity of nonlinear optics to interface magnetism, the relevance of substrate effects, and the enhanced potential of nonlinear spectroscopy, in particular for in-plane magnetized thin magnetic films in the monolayer range.

ACKNOWLEDGEMENTS We acknowledge computational vector optimization support by RZG, Garching (Munich), Germany, and financial support by the European Union TMR NOMOKE and DYNASPIN, Contract Nos. ERB-FMRX-CT96-0015 and ERB-FMRX-CT97-0124. We would like to thank Dr. R. Vollmer for his scrutiny in reading the manuscript.

REFERENCES

1 K.H. Bennemann (ed.): *Nonlinear Optics in Metals* (Clarendon, Oxford 1998)
2 B. Koopmans, M.G. Koerkamp, T. Rasing, H. van den Berg: Phys. Rev. Lett. **74**, 3692 (1995)
3 T. Rasing, M.G. Koerkamp, B. Koopmans, H. van den Berg: J. Appl. Phys. **79**, 6181 (1996)
4 T. Andersen, W. Hübner: Phys. Rev. B **65**, 174 409 (2002)
5 J.P. Dewitz, W. Hübner: Appl. Phys. B **68**, 491 (1999)
6 J.P. Dewitz, J. Chen, W. Hübner: Phys. Rev. B **58**, 5093 (1998)
7 A. Kirilyuk, V. Kirilyuk, T. Rasing: J. Magn. Magn. Mater. **198**, 620 (1999)
8 J. Reif, J.C. Zink, C.M. Schneider, J. Kirschner: Phys. Rev. Lett. **67**, 2878 (1991)
9 H.A. Wierenga, W. de Jong, M.W.J. Prins, T. Rasing, R. Vollmer, A. Kirilyuk, J. Kirschner: Phys. Rev. Lett. **74**, 1462 (1995)
10 H.A. Wierenga, M.W.J. Prins, D.L. Abraham, T. Rasing: Phys. Rev. B **50**, 1282 (1994)
11 R.-P. Pan, H.D. Wei, Y.R. Shen: Phys. Rev. B **39**, 1129 (1989)
12 W. Hübner, K.H. Bennemann: Phys. Rev. B **40**, 5973 (1989)
13 Y.Z. Wu, R. Vollmer, H. Regensburger, X.-F. Jin, J. Kirschner: Phys. Rev. B **63**, 054 401 (2001)
14 K.J. Veenstra, P.E. Hansen, A. Kirilyuk, A.V. Petukhov, T. Rasing: J. Magn. Magn. Mater. **198**, 695 (1999)
15 K. Sato, A. Kodama, M. Miyamoto, K. Takanashi, H. Fujimori, T. Rasing: J. Appl. Phys. **87**, 6785 (2000)
16 K. Sato, E. Taekada, M. Akita, M. Yamaguchi, K. Takanashi, S. Mitani, H. Fujimori, Y. Suzuki: J. Appl. Phys. **86**, 4985 (1999)
17 K. Takanashi, S. Mitani, H. Fujimori, K. Sato, Y. Suzuki: J. Magn. Magn. Mater. **177**, 1199 (1998)
18 A.V. Petukhov, I.L. Lyubchanskii, T. Rasing: Phys. Rev. B **56**, 2680 (1997)
19 I.L. Lyubchanskii, A.V. Petukhov, T. Rasing: J. Appl. Phys. **81**, 5688 (1997)
20 W. Hübner: Phys. Rev. B **42**, 11 553 (1990)
21 U. Pustogowa, W. Hübner, K.H. Bennemann: Phys. Rev. B **48**, 8607 (1993)
22 U. Pustogowa, W. Hübner, K.H. Bennemann: Phys. Rev. B **49**, 10 031 (1994)
23 W. Hübner, K.H. Bennemann, K. Böhmer: Phys. Rev. B **50**, 17 597 (1994)
24 A. Lessard, T.H. Moos, W. Hübner: Phys. Rev. B **56**, 2594 (1997)
25 B. Schulz, K. Baberschke: Phys. Rev. B **50**, 13 467 (1994)
26 P. Blaha, K. Schwarz, J. Luitz: *WIEN97, a Full Potential Linearized Augmented Plane Wave Package for Calculating Crystal Properties* (Karlheinz Schwarz, Wien 1999)
27 J.E. Sipe, D.J. Mooss, H.M. van Driel: Phys. Rev. B **35**, 1129 (1987)
28 D.W. Lynch, W.R. Hunter: in *Handbook of Optical Constants in Solids*, ed. by E.D. Palik (Academic, London 1985) pp. 275–367